Modification of North Atlantic Deep Water by Pacific/Upper Circumpolar Deep Water in the Argentine Basin

Sawyer V. S. Brand[1], Channing J. Prend[2], and Lynne D. Talley[3]

[1]University of Rhode Island
[2]Scripps Institution of Oceanography
[3]UCSD

November 22, 2022

Abstract

Much of the salty, high oxygen North Atlantic Deep Water (NADW) leaving the Atlantic flows through the Argentine Basin, where it is diluted by fresher, low oxygen Circumpolar Deep Water (CDW). This mixing of deep water masses is often overlooked in the zonally-averaged description of the overturning circulation. Here, we show that most of the mixing occurs along the western boundary: (i) extreme, isolated oxygen/temperature anomalies recorded by three autonomous biogeochemical floats suggest that subsurface eddies can inject relatively unmodified CDW far into the northwestern Argentine Basin, and (ii) moderate, numerous temperature/salinity anomalies indicate a mixing zone from Rio Grande Rise to the Malvinas Current. This western eddy pathway shortcuts the gyre-scale cyclonic route for CDW inferred from previous studies. Significantly, CDW dilution of NADW affects the properties of deep waters that upwell in the Southern Ocean, and hence the connection between Northern and Southern Hemisphere polar climates.

Modification of North Atlantic Deep Water by Pacific/Upper Circumpolar Deep Water in the Argentine Basin

S. V. S. Brand[1,2], C. J. Prend[2], and L. D. Talley[2]

[1]Scripps Institution of Oceanography, University of California San Diego, La Jolla, CA, USA
[2]University of Rhode Island, Narragansett, RI, USA

Corresponding author: Sawyer Brand (svbrand@uri.edu)

Key Points:

- Pacific/Circumpolar Deep Water with low oxygen, salinity, and pH dilutes North Atlantic Deep Water in the South Atlantic's Argentine Basin
- Isolated extreme low oxygen anomalies in the northwest Argentine Basin indicate a direct path of Circumpolar Deep Water northward via the Malvinas
- Strong isopycnic temperature variability along the western boundary identifies this as a mixing hotspot for these two deep water masses

Abstract

Much of the salty, high oxygen North Atlantic Deep Water (NADW) leaving the Atlantic flows through the Argentine Basin, where it is diluted by fresher, low oxygen Circumpolar Deep Water (CDW). This mixing of deep water masses is often overlooked in the zonally-averaged description of the overturning circulation. Here, we show that most of the mixing occurs along the western boundary: (i) extreme, isolated oxygen/temperature anomalies recorded by three autonomous biogeochemical floats suggest that subsurface eddies can inject relatively unmodified CDW far into the northwestern Argentine Basin, and (ii) moderate, numerous temperature/salinity anomalies indicate a mixing zone from Rio Grande Rise to the Malvinas Current. This western eddy pathway shortcuts the gyre-scale cyclonic route for CDW inferred from previous studies. Significantly, CDW dilution of NADW affects the properties of deep waters that upwell in the Southern Ocean, and hence the connection between Northern and Southern Hemisphere polar climates.

Plain Language Summary

Water, heat, and carbon are transported around the global ocean by the meridional overturning circulation, which helps regulate the climate system. In the Atlantic Ocean, the overturning circulation is characterized by net southward flow in the deep water layers, which transports water from the northern North Atlantic (North Atlantic Deep Water; NADW) all the way to the Southern Ocean. Often neglected in this picture is the modification of these deep waters as they flow south toward the Antarctic. Specifically, they become colder, fresher, and less oxygenated due to mixing with much older deep water from the South Pacific, which enters the Atlantic below South America and joins the Circumpolar Deep Water (CDW) flowing northward into the Argentine Basin. Here, using autonomous float measurements, we investigate the mixing between NADW and CDW in the Argentine Basin. We show that CDW can be transported far north on the western side of the basin in isolated subsurface eddies. Understanding these pathways is important because they influence the properties of the water that rises to the surface in the Southern Ocean; dilution of NADW by CDW damps the transmission of Northern Hemisphere climate change to the Southern Ocean.

1 Introduction

The Atlantic Meridional Overturning Circulation (AMOC) plays a key role in the climate system by redistributing heat, salt, and other tracers globally (e.g. McCarthy et al., 2015; Talley et al., 2011). The AMOC 'strength' is quantified from the net meridional transport as a function of latitude, subdivided into pressure or isopycnal layers (e.g. Lumpkin & Speer, 2007; Talley et al., 2003). The South Atlantic portion of the AMOC (SAMOC) consists of southward-flowing North Atlantic Deep Water (NADW) balanced by northward-flowing layers above and below—the thermocline/Antarctic Intermediate Water (AAIW)/Upper Circumpolar Deep Water (UCDW), and Lower Circumpolar Deep Water (LCDW)/Antarctic Bottom Water (AABW), respectively (e.g. Ganachaud & Wunsch, 2000; Garzoli & Matano, 2011; Hernandez-Guerra et al., 2019; Lumpkin & Speer, 2007; Schmitz, 1995; Talley et al., 2003; Wüst, 1935).
However, this zonally-integrated view of the AMOC obscures significant lateral variations in transport within each layer (e.g. Hernández-Guerra et al., 2019; Reid, 1989). Particularly for the AMOC's intermediate and deep layers, lateral circulation is often neglected despite its role in juxtaposing different water masses and hence modifying their properties. Such exchanges have

been articulated and quantified in the North Atlantic as central to the evolution of tracer ages along the Deep Western Boundary Current (DWBC) (Rhein et al., 2015) and at high latitudes (McCartney, 1992).

Similarly, in the South Atlantic, the net southward transport of 'NADW' (potential density range σ_2 = 36.65 to 36.9 kg m^{-3}) is more precisely the residual between southward-flowing NADW and northward-flowing CDW. The geostrophic circulation and interleaving of these deep waters were mapped and described by Reid (1989, 1994), and are depicted schematically in Figure 1. In the subtropical South Atlantic, NADW first branches eastward from the DWBC in the Brazil Basin but most continues southward into the Argentine Basin before entering the Antarctic Circumpolar Current (ACC) (Stramma & England, 1999; Garzoli & Matano, 2011). Garzoli et al. (2015) calculate that almost 80% of the NADW transport follows the latter pathway through the Argentine Basin, which is consistent with Lagrangian particle release experiments in Tamsitt et al. (2017).

Once in the Argentine Basin, the salty, high oxygen NADW meets CDW that enters from the south via the Malvinas Current, which arises from the Subantarctic Front in Drake Passage (Campos et al., 1995) (Figure 1). CDW contains a large component of fresher, low oxygen Pacific Deep Water (PDW) from the southeast Pacific. Abyssal eddies containing relatively unmodified LCDW have been observed from multiple hydrographic surveys in the western Argentine Basin (Arhan et al., 2002; Gordon & Greengrove, 1986) (green squares in Figure 2). The contrast between NADW and CDW has been readily apparent as far back as Wüst (1935) (see Supplementary Figure S1) and culminates in a reduction of oxygen in waters identified as NADW in the Argentine Basin (Jullion et al., 2010).

In this study, we use data from core and biogeochemical (BGC) Argo floats to reassess the interaction between NADW and CDW in the SAMOC. We find isolated anomalies of oxygen, temperature, and salinity in the deep water density range that indicate penetration of unmixed CDW far into the northern Argentine Basin. While vigorous eddies are found throughout the region (e.g. Mason et al., 2017), mixing between NADW and CDW occurs primarily along the western boundary, where the water masses meet and their contrast is greatest. This dilution of NADW by CDW is more than a regional curiosity; when NADW reaches the Southern Ocean, it upwells to the sea surface and acts as a conduit between Northern and Southern Hemisphere polar climates (e.g. Adkins, 2013; Buizert et al., 2015). The admixture of older PDW-dominated CDW thus damps the transmission of Northern climate change to the Southern Ocean.

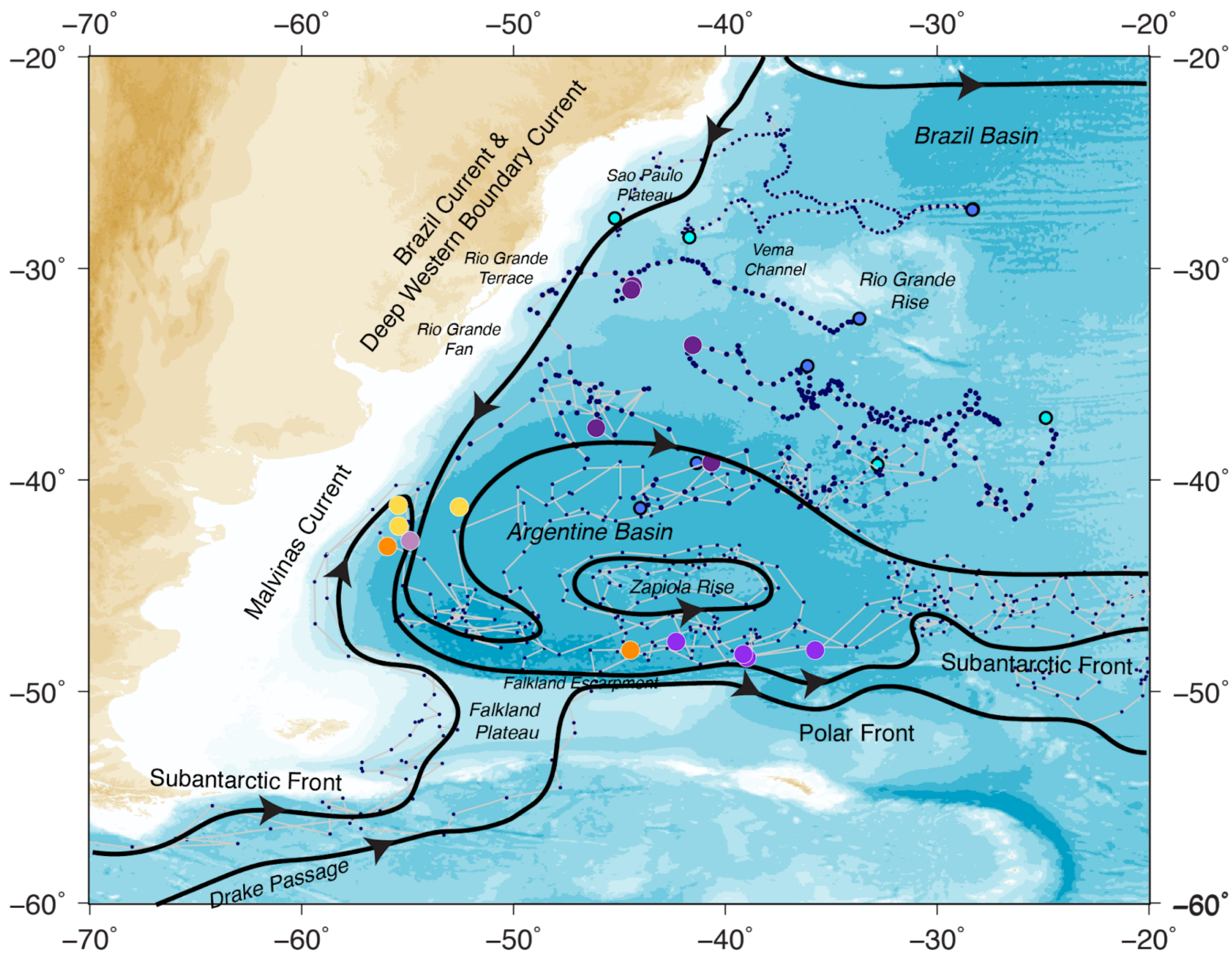

Figure 1. Schematic of Argentine Basin deep water circulation, based in part on Reid (1989) and Valla et al. (2018). Dark purple circles are the locations of anomalously low oxygen measured by SOCCOM BGC Argo floats (Fig. 2). Lighter purple circles show the locations of additional anomalously low oxygen profiles in the southern Argentine Basin. Yellow and orange circles mark anomalously high oxygen profiles. The 5 SOCCOM floats deployed on the RRS James Clark Ross AMT28 expedition in 2018 are shown (first profile: medium blue dots; last profile: medium cyan dots; all others: small dots; floats with anomalous oxygen shown with slightly larger small dots). The profile locations reflect data available through Jan. 21, 2022. Three additional SOCCOM floats deployed in northern Drake Passage and the southeast Pacific are also shown. See Supplementary Figures S2 and S4 for trajectories and oxygen profiles.

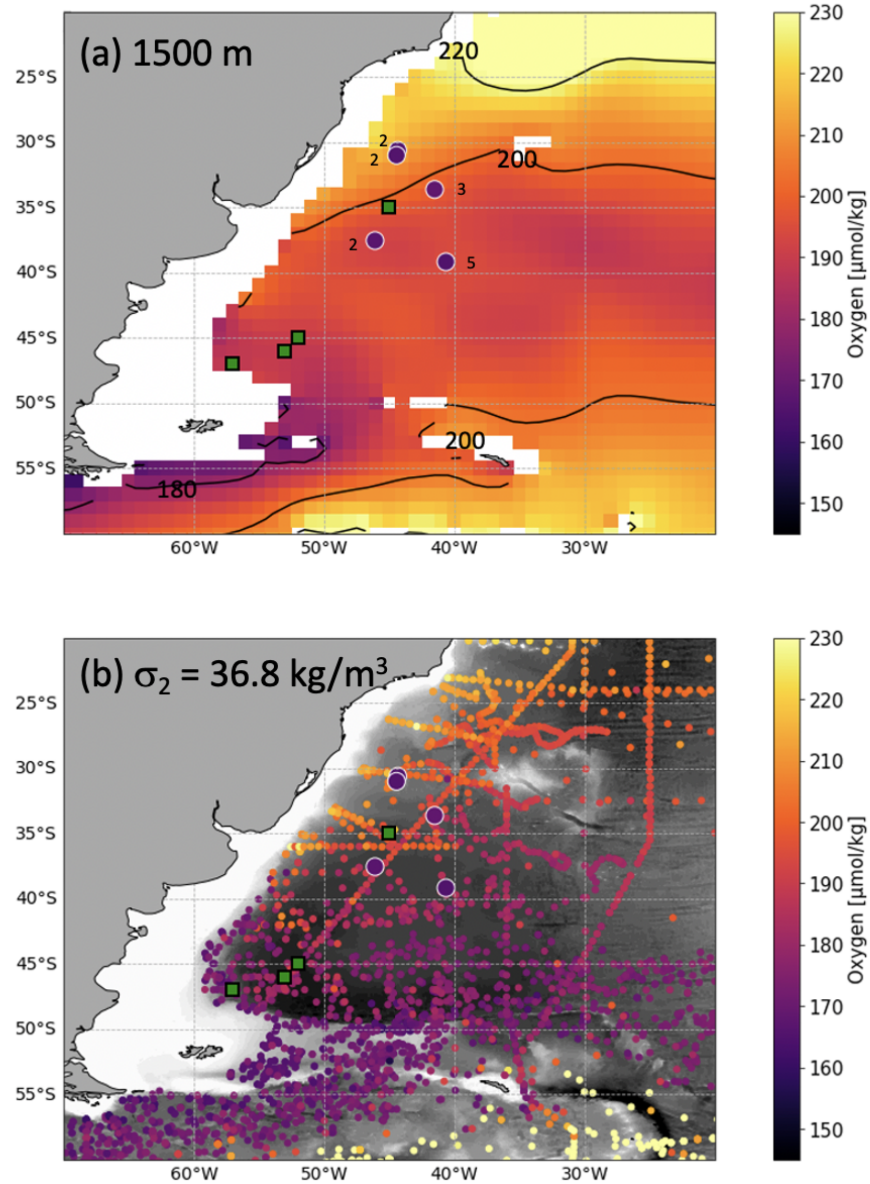

Figure 2. Dissolved oxygen in the upper deep water layer. (a) World Ocean Atlas 2018 (WOA18) dissolved oxygen climatology at 1500 m for the Atlantic (Garcia et al., 2018). (b) Oxygen from historical hydrographic station profiles from NODC (2005), SOCCOM Biogeochemical Argo float profiles (years 2015-2021), and quality-controlled oxygen Argo floats (Drucker and Riser, 2016), interpolated to potential density surface σ_2 = 36.8 kg m^{-3}. Locations of profiles with anomalous oxygen in both panels from the three SOCCOM floats (WMOID 5905983, 5905985, and 5905982) are shown as large circles colored by dissolved oxygen at σ_2 = 36.8 kg m^{-3}. Green squares in both panels are locations of much deeper eddies identified by Gordon & Greengrove (1986) and Arhan et al. (2002).

2. Data and Methods

2.1 Float and Shipboard Profile Data

Our analysis uses in-situ measurements from autonomous profiling floats deployed by the Argo and Southern Ocean Carbon and Climate Observations and Modeling (SOCCOM) programs. Core Argo is a global array consisting of approximately 4000 floats that measure temperature, salinity, and pressure in the upper 2000 m of the water column every 10 days (Roemmich et al., 2019). Here, we analyze 116,029 delayed-mode, quality controlled profiles collected in and around the Argentine Basin (60°S to 10°S, 10°W to 70°W) from 1998 to 2020. For each profile, we calculate conservative temperature, absolute salinity, and potential density referenced to 2,000 m (σ_2) using the Gibbs seawater (GSW) package routines (http://www.teos-10.org). All fields are then linearly interpolated to a uniformly-spaced potential density axis with 0.01 kg m^{-3} resolution.

SOCCOM has deployed more than 200 Argo-equivalent BGC floats in the Southern Ocean since 2014. SOCCOM floats measure dissolved oxygen, nitrate, pH, fluorescence, and backscatter, in addition to temperature and salinity, with the same sampling frequency and vertical coverage as core Argo. The quality-controlled data from the September 1, 2021 SOCCOM snapshot are used in this analysis (Johnson et al., 2021). Here, we analyze 1118 SOCCOM profiles from 2016 to the present; these include data from 4 floats that were deployed in the Argentine Basin during the 2018 Atlantic Meridional Transect Program (AMT28) (Tarran, 2018) as well as 14 other SOCCOM floats that drifted into the region from the South Pacific or from the eastern South Atlantic. We also use 206 profiles from non-SOCCOM, oxygen-equipped Argo floats deployed by the University of Washington between 2003 and 2014 (Drucker and Riser, 2016).

In addition to the float data, we utilize the World Ocean Atlas 2018 dissolved oxygen climatology at 1°×1° resolution (Garcia et al., 2018) to plot the climatological mean oxygen at 1500 m (Figure 2a), which is the approximate depth of the 36.8 σ_2 level that represents the UCDW oxygen minimum and anomalies in the Argentine Basin. Individual hydrographic station data are used in Figure 2b to display oxygen on the isopycnal; this curated dataset was collated in the early 2000s from Reid's (1994) quality-controlled datasets, augmented by WOCE Hydrographic Program data and other high quality hydrography of the 1980s and 1990s. A total of 610 stations in the Argentine Basin are used here.

2.2 Argo Temperature and Salinity Anomalies

In Section 3, we present large oxygen anomalies, in the deep water density range, observed from SOCCOM profiles, which are also associated with anomalous temperature, salinity, and pressure. To investigate the prevalence of such anomalies, we compute temperature and salinity statistics from core Argo, which provides a much larger dataset than the SOCCOM floats. Conservative temperature (T), absolute salinity (S), and pressure (P) from all available core Argo profiles were interpolated to isopycnal surfaces as described above; Figure 4a,c shows the profile locations, colored by temperature and pressure on the 36.8 σ_2 level. All fields were then bin-averaged to a 1°×1° grid (Supplementary Figure S5), and for each profile, T, S, and P anomalies were defined relative to the local bin average (Figure 4b,d). These anomalies highlight locations with significant along-isopycnal variability.

3. UCDW Oxygen Anomalies

The contrast between NADW and CDW is illustrated by oxygen on deep isopycnal and pressure surfaces (Figure 2; Supplementary Figure S1). Namely, low oxygen marks the core of UCDW due to its origin as old Pacific and Indian Deep Water. Salinity also distinctly characterizes NADW and CDW (e.g. Talley, 2013), but the high salinity core of NADW sits below the maximum depth of Argo coverage (i.e. 2000 m). In the Argentine Basin, higher oxygen concentrations occur at the western boundary where NADW penetrates southward. The lowest oxygen values are observed in the southern Argentine Basin, where UCDW crosses the Falkland Plateau in both the Subantarctic and Polar Fronts (Figure 1).

The oxygen climatology at 1500 m (Figure 2a) shows concentrations between 180 and 200 μmol/kg throughout the Argentine Basin, except in the northern DWBC where it is higher. However, this smoothed field obscures significant deep variability. For example, south of the Brazil-Malvinas Confluence (BMC) at 40°S, the individual hydrographic station profiles at $\sigma_2 = 36.8$ (Figure 2b) reveal lower oxygen in the Malvinas with patchy higher oxygen offshore where Brazil Current water extends towards Zapiola Rise (Figure 1). North of the BMC, isolated profiles of higher oxygen (orange/yellow) suggest southward movement of NADW along the western boundary, while isolated profiles of lower oxygen (darker purple) indicate penetration of UCDW as far north as 37°S at the western boundary and 30°S offshore.

In the northern Argentine Basin, the 5 large purple dots in Figures 1 and 2 indicate individual SOCCOM float profiles with anomalously low dissolved oxygen concentrations in the deep water density range ($\sigma_2 = 36.65$ to 36.9) (Figure 3). Their oxygen concentrations ranged from 12 to 52 μmol/kg lower than the other profiles measured by these floats, which is 2 to 8 times the standard deviation (Figure 3 and Supplementary Table S1). These extreme oxygen anomalies were also associated with anomalously low temperature and salinity (Figure 3), and with high nitrate and low pH (Supplementary Figure S3), and thus are unlikely to be due to sensor malfunction. Each anomaly has a striking vertical structure, with an abrupt break in the profile at the top of the anomaly in physical space (Supplementary Figure S3), occurring between 1000 to 1700 m, and at densities of $\sigma_2 = 36.6$ to 36.8 (Supplementary Table S1). Note that because Argo profiles are limited to 2000 m, the bottom of the anomalies cannot be characterized.

The density, oxygen concentration, and temperature of these anomalies are consistent with UCDW, whose principal source in the Argentine Basin is the southeast Pacific Ocean's oxygen-poor PDW. PDW enters the Atlantic through Drake Passage and then follows the Malvinas Current northward (Supplementary Figure S1). Circulation schematics often feature an anticyclonic pathway of CDW around the Argentine Basin (e.g. Stramma and England, 1999; Valla et al., 2018), following the dominant route for the overlying AAIW (Reid, 1989). However, CDW is constantly mixing with ambient waters along this pathway and thus would be strongly modified along such a circuitous route to the northwestern Argentine Basin where the anomalous profiles were found. Therefore, the anomalies most likely moved directly northward from the BMC. This is supported by Reid's (1989, 1994) circulation at 1500 to 2500 m, and is the basis for our Figure 1 schematic.

The unusual abrupt vertical layering of northern and southern water masses in these anomalous profiles indicates relatively pure sources of each. To reach the location of the northernmost anomalies, this means that unadulterated oxygen-poor CDW must propagate 500 to 1000 km from its nearest source at the BMC. This could be accomplished by coherent subthermocline eddies, which do not easily mix with surrounding water. The abruptness of the anomalous profile breaks indicates local layering/intrusions. However, the layer breaks are not at uniform depths or densities (~1300 to 1600 m depth, Figure 3). This suggests bathymetry-following southward flow of NADW that is forced offshore by the topography and then into or over eddies containing purer CDW. Indeed, float 5905982 followed just such a pathway offshore from the Brazil Current into an eddying field (Supplementary Figure S2), and notably recorded 3 of the 5 SOCCOM low oxygen anomalies.

Given that we only have single profiles, we cannot unequivocally say that the oxygen anomalies are due to coherent subthermocline vortices, although they are associated with small negative pressure anomalies (Figure 3), suggesting that they are cyclonic. Furthermore, Gordon & Greengrove (1986) and Arhan et al. (2002) have previously documented much deeper subthermocline eddies containing the much denser LCDW in the Argentine Basin (green squares in Figures 1, 2, and 4), using tightly spaced hydrographic stations. Arhan et al. (2002) hypothesized that these deep eddies originated from destabilization of the deep Malvinas Current, at a point along the Malvinas Loop. The northernmost eddy identified by Arhan et al. (2002) is co-located with the cluster of SOCCOM oxygen anomalies.

In addition to the 5 anomalous oxygen profiles discussed above, several other prominent anomalies were observed in the southern Argentine Basin (Figure 1 and Supplementary Table S2). For example, multiple low oxygen anomalies in the eastward flow between Zapiola Rise and the Falkland Escarpment likely resulted from the movement of UCDW across the Falkland Plateau with the Polar Front. These contribute to CDW/NADW mixing along the Subantarctic Front, but are unlikely to circulate northwestward into the northern Argentine Basin. Several high oxygen anomalies (Figure 1, Supplementary Figure S4b, d) were located in the BMC, where NADW and CDW meet head-on. Finally, a high oxygen anomaly, which would be NADW from the Brazil Current, was found near the southwestern side of Zapiola Rise (Supplementary Figure S4f), where historical oxygen data also suggest such anomalies (Figure 2b).

Profiles with these anomalous structures are striking because of their relative rarity, constituting only a handful of the total 1118 SOCCOM BGC profiles in the Argentine Basin. This is perhaps surprising given how eddy-rich the region is (Juillon et al., 2010; Piola and Matano, 2017), which may indicate that the energetic mixing between water masses proceeds at the smaller vertical finestructure scale of 10-100 m documented by Bianchi et al. (1993).

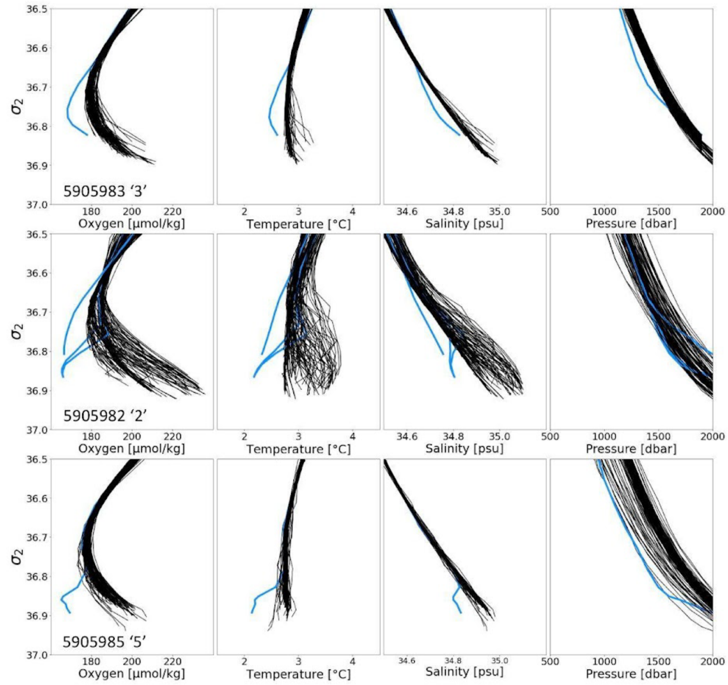

Figure 3. All profiles from the three SOCCOM BGC Argo floats with anomalously low oxygen values in the northern Argentine Basin. (Left) Dissolved oxygen, (center left) conservative temperature, (center right) absolute salinity, and (right) pressure profiles from floats 5905983 (top), 5905982 (middle), and 5905985 (bottom). Profiles that are anomalously low in dissolved oxygen relative to the σ_2 = 36.65-36.85 kg m^{-3} isopycnal layer are shown in blue (locations in Fig. 2, labeled by float abbreviations shown here in quotes). Profile locations are shown in Supplementary Figure S2.

4. Deep Water Eddy Field

The extreme but scarce anomalies reported in Section 3 are due to interleaving of NADW and CDW in the circulation and eddy field of the Argentine Basin. Since the oxygen anomalies are also associated with anomalous temperature and salinity (Figure 3), we turn to the much larger core Argo dataset for a more comprehensive view of the water mass juxtaposition. As described in Section 2.2, we interpolated temperature, salinity, and pressure (T, S, P) onto isopycnal surfaces. Figure 4a,c shows T and P on the 36.8 σ_2 surface, which lies in the core of the UCDW oxygen minimum layer. By 'NADW' for this isopycnal, we refer to the warm, salty, oxygenated water originating in the north, but which lies above the NADW core's salinity maximum, which itself is below the Argo depth range of 2000 m. We then bin average the T and P values (Figure S5), and calculate the anomaly for each profile relative to the local mean (Figure 4b,d).

The temperature distribution at σ_2 = 36.8 (Figure 4c and Supplementary Figure S5c) has a strong meridional gradient. Namely, warm NADW from the north enters the Argentine Basin in the DWBC, while cool CDW from Drake Passage crosses the Falkland Plateau and flows equatorward in the Malvinas Current. The pressure at σ_2 = 36.8 (Figures 4a and S5a) is 1200 to 1800 dbar in the Argentine and Brazil Basins. Note that the isopycnal rises steeply across the Polar Front indicating outcropping within the ACC; however this outcropped water has limited impact on Argentine Basin UCDW. Within the Argentine Basin, the subtler patterns of temperature and pressure variability at $\sigma_2 = 36.8$(Fig. 4c) are relevant to the extreme oxygen anomalies. Just after the warm DWBC moves southward past Sao Paulo Plateau, it spawns an eastward excursion of warmer water around 33°S. The 3 northernmost extreme oxygen anomalies (purple circles) are located in this eastward plume.

Regions with significant along-isopycnal variability are marked by large anomalies (relative to the local bin average) in Figure 4b,d. The largest temperature anomalies (Figure 4d) form a striking pattern along the offshore side of the warm western boundary waters. This is the mixing front (water mass front) between NADW and UCDW. Hotspots of anomalies appear at 40°S in the BMC, and at the entry location of the DWBC to the Argentine Basin over the Sao Paulo Plateau. (Farther north in the Brazil Basin, the strong anomalies extend eastward in a band around 20°S to 25°S, marking the local eastward flow of NADW from the DWBC.) The standard deviations of temperature within the 1°×1° bins (Supplementary Figure S5d) also highlight the very high variability along the water mass front and at the BMC.

Strong isopycnic T anomalies require both a large water mass contrast and a dynamic eddy field. The eddy field, in turn, is represented by isopycnic P anomalies (Figure 4b), which indicate locations with significant vertical excursions of the isopycnal. The highest P anomalies are found at the western boundary in the Malvinas and DWBC, and along the Falkland Escarpment to the south. High P variability also occurs where the Brazil and Malvinas Current fronts split around Zapiola Rise (Figure 1 schematic based on Reid, 1989), and to the east of the Rise where these flows rejoin. This overall pattern, of a ‘donut’ of high variability in the Argentine Basin with weak variability over Zapiola Rise and in the Brazil Basin, strongly resembles surface eddy kinetic energy from altimetry (e.g. Mason et al., 2017; Yu et al., 2018).

It is important to realize that large pressure and temperature anomalies are not necessarily co-located. In other words, dynamical and water mass variability patterns differ (Figures 4b, d). Along-isopycnal temperature variability in the Argentine Basin is highest along the western boundary where there is both a CDW/NADW water mass front and high pressure variability. However, in the zonal portions of the Argentine Basin’s ‘donut’ of high pressure variability and thus high eddy activity, temperature variability is low because of the absence of a water mass contrast. Finally, temperature variability is high in the southern Brazil Basin, where there is a strong zonal CDW/NADW boundary (Figure 4c) but little pressure variability (Figure 4b).

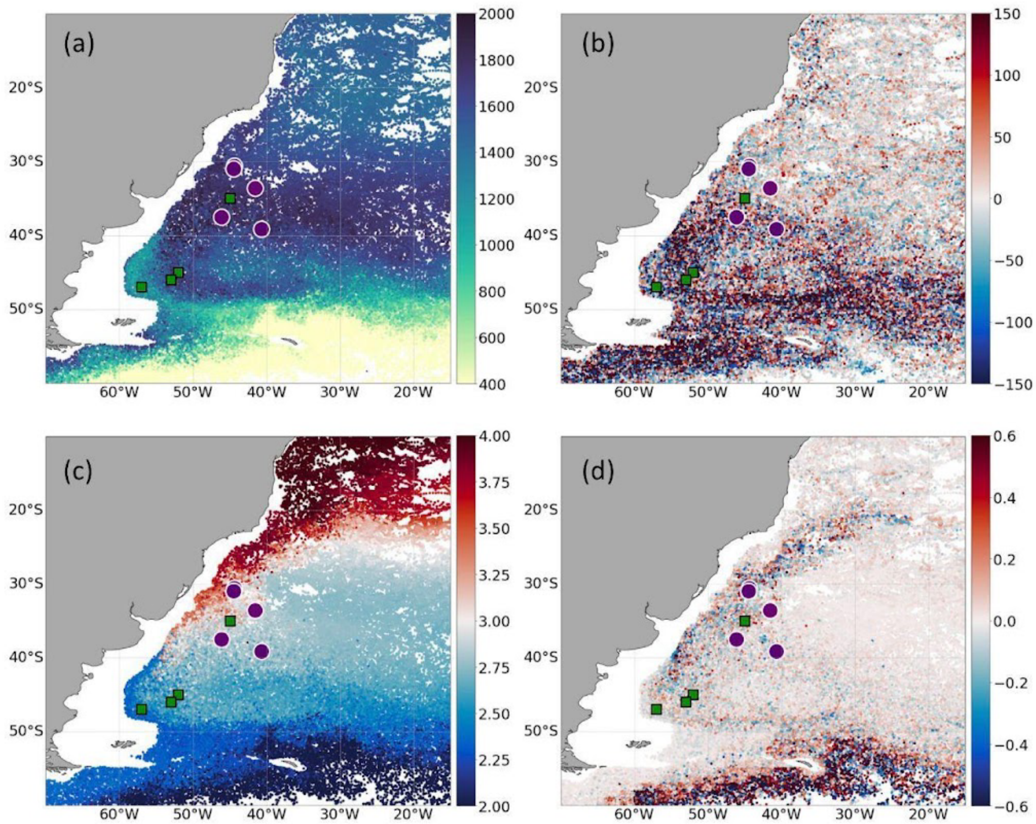

Figure 4. Pressure and temperature on the σ_2 = 36.8 kg m^{-3} surface from all Argo profiles (years 1998 - 2020). (a) Pressure for each profile, (b) pressure anomaly (dbar) from the bin average for each profile, (c) conservative temperature (°C) for each profile, and (d) conservative temperature anomaly (°C) from the bin average for each profile. The mean pressure and temperature were averaged in 1°x1° lat/lon bins, shown in Supplementary Figure S5, along with their standard deviations. The SOCCOM float profiles with large oxygen anomalies are shown with their oxygen contour colors from Figure 2. Green squares denote previously-identified near-bottom eddies.

5 Conclusions

In discussions of the MOC, the focus is usually on the fate of the ventilated, sinking components from the Northern Hemisphere that produce NADW and from the Southern Hemisphere that produce AABW/LCDW. These carry the history of surface conditions from their formation regions to the upwelling regions of the global ocean, mostly within the ACC and to its south. Often lost in this simplified view of the MOC is the modification of these waters, particularly NADW, as they traverse their overturning pathways. Once NADW leaves the mid-latitude North Atlantic and is advected southward, its properties are mostly maintained until it reaches the mid-latitude South Atlantic. Previous studies have shown that almost 80% of the southward NADW transport goes through the Argentine Basin (Garzoli et al., 2015), a region with significant deep and abyssal variability (Kersale et al., 2021). TWe note though that the high salinity, high oxygen signature of NADW weakens almost immediately upon entry into the region near the Sao Paulo Plateau at about 30°S (Figure 1). As the NADW flows further southward in the Argentine Basin, it is further modified until it encounters the Malvinas Loop (Figure 2). The modified NADW turns to flow eastward both north and south of Zapiola Rise and then joins the eastward circumpolar flow.

This significant modification of NADW in the Argentine Basin is due to mixing with CDW, both at the depth of the NADW core and sandwiching it above and below. We have shown, using the sparse BGC Argo data set, augmented with historical hydrographic data, that nearly unadulterated CDW is found sporadically in the northwestern Argentine Basin. These extreme, isolated oxygen anomalies reveal an important pathway northward from the Malvinas Loop, rather than the more circuitous counterclockwise path around the full South Atlantic depicted in many previous schematics. Moreover, these isolated anomalies are located where we have shown that temperature/salinity variability is large on NADW/CDW isopycnals, based on the larger core Argo data set. Hence the primary mixing interface between NADW and CDW is within the western boundary currents. Notably, a strong eddy field is a necessary condition for mixing of the water masses, but it is not sufficient – strong dilution of NADW also requires the water mass contrast created by the northward shortcut of CDW in this western region.

Why is it important to document the mixing between deep waters? When NADW enters the Southern Ocean, its properties are informed by surface processes in the northern North Atlantic about 200 years earlier, as well as the modification that occurs through mixing as these waters traverse the length of the Atlantic. This modification is most extreme in the Argentine Basin due to CDW, whose low oxygen, high carbon, and low pH (e.g. Supplementary Figure S3) result from its aged components; PDW age exceeds 1000 years. These time scales could lead to higher carbon outgassing potential in PDW/CDW than in NADW (Chen et al., submitted). But by the time NADW enters the Southern Ocean and upwells to the sea surface, it has been diluted by mixing with carbon-rich CDW, and therefore is nearly equally capable of outgassing at the sea surface (Bushinsky et al., 2019; Prend et al., submitted). If the dilution rate depends on fluctuations in the Malvinas and Brazil/Deep Western Boundary Current transports and eddy fields, then changes in forcing on climatic time scales could alter the properties of the upwelled deep waters and associated air-sea gas exchange.

Here we have seen that the expanding BGC float sampling of the western South Atlantic, almost equal in just 3 years to the historical ship-based data set, is revealing deep water property anomalies that clarify understanding of the juxtaposition and mixing of the globally-important CDW and NADW. The 17 years of Argo profiling in the same region provides a comprehensive geographic view of the mixing of these deep waters. Both reveal the importance of the western boundary region of the Argentine Basin for southward and northward transport. The expected continued BGC float sampling in the subtropical South Atlantic will eventually allow dense mapping of BGC anomalies similar to the temperature/salinity fields, and hence improved quantification of BGC property dilution as it reaches the Southern Ocean.

Acknowledgments

We acknowledge our SOCCOM program colleagues for production of BGC floats and data processing since 2014, and for years of scientific discussion. We thank G. Tarran and the science party of Plymouth Marine Laboratory for deploying the Argentine Basin SOCCOM floats during the AMT28 project on the RRS James Clark Ross (https://www.amt-uk.org/Cruises/AMT28). SVSB, LDT and CJP were supported by NSF PLR-1425989 to the

SOCCOM program. CJP was also supported by a National Science Foundation Graduate Research Fellowship under grant DGE-1650112.

Open Research

BGC profiling float data were collected and made freely available by the Southern Ocean Carbon and Climate Observations and Modeling (SOCCOM) Project funded by the National Science Foundation, Division of Polar Programs (NSF PLR -1425989), supplemented by NASA, and by the International Argo Program and the NOAA programs that contribute to it. (http://www.argo.ucsd.edu, http://argo.jcommops.org). The Argo Program is part of the Global Ocean Observing System. All SOCCOM data are available through the Argo GDACs. Calibrated SOCCOM data from the April 20, 2020 snapshot (doi.org/10.6075/J0KK996D) were used here, which is available at https://soccompu.princeton.edu/www/index.html.

The calibrated Argo oxygen data from Drucker and Riser (2016) are available at https://soccom.princeton.edu/content/uw-global-o2-data-set; these data are also part of the complete Argo data set, as above.

Shipboard hydrographic data were collected by the World Ocean Circulation Experiment (WOCE) and numerous other selected research cruises spanning many decades. All data are available from the NCEI World Ocean Database (WOD) (https://www.ncei.noaa.gov/access/world-ocean-database-select/dbsearch.html) and were quality controlled by J. L. Reid (Reid, 1994) and co-author LDT.

The oxygen climatology based on historical hydrographic data is from the World Ocean Atlas 2018 (Garcia et al., 2018), and is available at https://www.ncei.noaa.gov/access/world-ocean-atlas-2018/.

References

Adkins, J. (2013), The role of deep ocean circulation in Glacial to Interglacial climate change. *Paleoceanography, 28*, 1-23, doi:10.1002/palo.20046

Arhan, M., Carton, X., Piola, A., & Zenk, W. (2002), Deep lenses of circumpolar water in the Argentine Basin. *Journal of Geophysical Research: Oceans*, *107*(C1), 7-1.

Bianchi, A. J., Giulivi, C. F., & Piola, A. R. (1993), Mixing in the Brazil-Malvinas confluence. *Deep-Sea Research I, 40*(7), 1345-1358.

Buizert, C., Adrian, B., Ahn, J., Albert, M., Alley, R. B., Baggenstos, D., …, & Woodruff, T. E. (2015), Precise interpolar phasing of abrupt climate change during the last ice age. *Nature, 520*, 661–665. https://doi.org/10.1038/nature14401

Bushinsky, S. M., Landschützer, P., Rödenbeck, C., Gray, A. R., Baker, D., Mazloff, M. R., et al. (2019), Reassessing Southern Ocean air-sea CO2 flux estimates with the addition of biogeochemical float observations. *Global Biogeochemical Cycles, 33*, 1370–1388. https://doi.org/10.1029/2019GB006176

Campos, E. J., Velhote, D., & da Silveira, I. C. (2000), Shelf break upwelling driven by Brazil Current cyclonic meanders. *Geophysical Research Letters*, *27*(6), 751-754.

Chen, H., Haumann, F.A., Talley, L.D., Johnson, K.S., & Sarmiento, J. (2022), The deep ocean's carbon exhaust. *Global Biogeochemical Cycles*, submitted.

Drucker, R., & Riser, S. C. (2016), In situ phase-domain calibration of oxygen Optodes on profiling floats. *Methods in Oceanography*, *17*, 296-318.

Ganachaud, A., & Wunsch, C. (2000), Improved estimates of global ocean circulation, heat transport and mixing from hydrographic data. *Nature, 408*, 453–457.

Garcia, H. E., Weathers, K., Paver, C. R., Smolyar, I., Boyer, T. P., Locarnini, R. A., … & Reagan, J. R. (2018), *World Ocean Atlas 2018, Volume 3: Dissolved Oxygen, Apparent Oxygen Utilization, and Oxygen Saturation*. A. Mishonov Technical Ed.; NOAA Atlas NESDIS 83, 38pp.

Garzoli, S. L., Dong, S., Fine, R., Meinen, C. S., Perez, R. C., Schmid, C., van Sebille, E., & Yao, Q. (2015), The fate of the Deep Western Boundary Current in the South Atlantic. *Deep Sea Research Part I, 103,* 125-136. http://dx.doi.org/10.1016/j.dsr.2015.05.008

Garzoli, S. L., & Matano, R. (2011), The South Atlantic and the Atlantic meridional overturning circulation. *Deep Sea Research Part II: Topical Studies in Oceanography*, *58*(17-18), 1837-1847.

Gordon, A. L., & Greengrove, C. L. (1986), Geostrophic circulation of the Brazil-Falkland confluence. *Deep Sea Research Part A. Oceanographic Research Papers*, *33*(5), 573-585.

Hernández-Guerra, A., Talley, L., Pelegri, J. L., Velez-Belchi, P., Baringer, M. O., Macdonald, A., & McDonagh, E. L. (2019), The upper, deep, abyssal and overturning circulation in the Atlantic Ocean at 30S in 2003 and 2011. *Prog in Oceanogr., 176 (102136)*, 1-24. https://doi.org/10.1016/j.pocean.2019.102136

Johnson, K. S., Riser, S. C., Boss, E. S., Talley, L. D., Sarmiento, J. L., Swift, D. D., …, & Russell, J. L.. (2021), SOCCOM float data - Snapshot 2021-09-21. In *Southern Ocean Carbon and Climate Observations and Modeling (SOCCOM) Float Data Archive*. UC San Diego Library Digital Collections. https://doi.org/10.6075/J0CF9Q81

Jullion, L., Heywood, K. J., Naveira Garabato, A. C., & Stevens, D. P. (2010), Circulation and water mass modification in the Brazil–Malvinas Confluence. *Journal of Physical Oceanography*, *40*(5), 845-864. https://journals.ametsoc.org/view/journals/phoc/40/5/2009jpo4174.1.xml

Kersale, M., Meinen, C. S., Perez, R. C., Le Henaff, M., Valla, D., Lamont, T., ... & Garzoli, S. L. (2020), Highly variable upper and abyssal overturning cells in the South Atlantic. *Science Advances*, *6*(32), eaba7573.

Lumpkin, R., & Speer, K. (2007), Global ocean meridional overturning. *J. Phys. Oceanogr. 37*, 2550-2562.

Mason, E., Pascual, A., Gaube, P., Ruiz, S., Pelegrí, J. L., & Delepoulle, A. (2017), Subregional characterization of mesoscale eddies across the Brazil-Malvinas Confluence. *J. Geophys. Res. Oceans*, *122*, 3329– 3357. doi:10.1002/2016JC012611

McCarthy, G. D., Smeed, D. A., Johns, W. E., Frajka-Williams, E., Moat, B. I., Rayner, D., ... & Bryden, H. L. (2015), Measuring the Atlantic meridional overturning circulation at 26 N. *Progress in Oceanography*, *130*, 91-111.

McCartney, M. S. (1992), Recirculating components to the deep boundary current of the northern North Atlantic. *Progress in Oceanography, 29*, 283-383.

NODC (2005), World Ocean Database 2005 (WOD05). NOAA National Oceanographic Data Center. http://www.nodc.noaa.gov/OC5/WOD05/pr_wod05.html

Piola, A.R., Matano, R.P., (2017). Ocean currents: Atlantic western boundary—Brazil current/Falkland (Malvinas) current. *Encyclopedia of Ocean Sciences (Third Edition). Reference module in Earth Systems and Environmental Sciences*, Elsevier, doi: https://doi.org/10.1016/B978-0-12-409548-9.10541-X

Prend, C.J., Gray, A.R., Talley, L.D., Gille, S.T., Haumann, F.A., Johnson, K.S., Riser, S.C., Rosso, I., Sauve, J., & Sarmiento, J.L. (2022), Indo-Pacific sector dominates Southern Ocean carbon outgassing. *Global Biogeochemical Cycles*, submitted.

Reid, J. L. (1989), On the total geostrophic circulation of the South Atlantic Ocean: Flow patterns, tracers and transports. *Progr. Oceanogr., 23*, 149-244.

Reid, J. L. (1994), On the total geostrophic circulation of the North Atlantic Ocean: Flow patterns, tracers and transports. *Progr. Oceanogr., 33*, 1-92.

Rhein, M., Kieke, D., & Steinfeldt, R. (2015), Advection of North Atlantic Deep Water from the Labrador Sea to the southern hemisphere. *J. Geophys. Res. Oceans, 120*, 2471–2487, doi:10.1002/2014JC010605

Roemmich, D., Alford, M. H., Claustre, H., Johnson, K., King, B., Moum, J., ... & Yasuda, I. (2019), On the future of Argo: A global, full-depth, multi-disciplinary array. *Frontiers in Marine Science*, *6*, 439.

Schmitz, W. J. (1995), On the interbasin-scale thermohaline circulation. *Rev. Geophys. 33,* 151-173.

Stramma, L., & England, M. (1999), On the water masses and mean circulation of the South Atlantic Ocean. *Journal of Geophysical Research: Oceans*, *104*(C9), 20863-20883.

Talley, L. D. (2013), Closure of the global overturning circulation through the Indian, Pacific, and Southern Oceans: Schematics and transports. *Oceanography*, *26*(1), 80-97.

Talley, L. D., Pickard G.L., Emery W.J., & Swift J.H. (2011), *Descriptive Physical Oceanography: An Introduction (Sixth Edition)*. Elsevier, Boston, 560 pp.

Talley, L. D., Reid, J. L., & Robbins, P. E. (2003), Data-based meridional overturning streamfunctions for the global ocean. *J. Climate, 16*, 3213-3226.

Tamsitt, V., Drake, H., Morrison, A. K., Talley, L. D., Dufour, C. O., Gray, A. R., …, & Weijer, W. (2017), Spiraling up: pathways of global deep waters to the surface of the Southern Ocean. *Nature Comm., 8*, doi:10.1038/s41467-017-00197-0.

Tarran, G. (2018), AMT 28 Cruise Report: RRS James Clark Ross (JR18-001). Atlantic Meridional Transit Project Office, Plymouth Marine Laboratory. https://www.amt-uk.org/getattachment/Cruises/AMT28/AMT_28_CRUISE_REPORT_RS.pdf (accessed 15 Jan. 2022).

Valla, D., Piola, A. R., Meinen, C. S., & Campos, E. (20189), Abyssal transport variations in the southwest South Atlantic: First insights from a long-term observation array at 34.5 S. *Geophysical Research Letters*, *46*(12), 6699-6705.

Wüst, G., 1935. Schichtung und Zirkulation des Atlantischen Ozeans. Die Stratosphäre. In Wissenschaftliche Ergebnisse der Deutschen Atlantischen Expedition auf dem Forschungs- und Vermessungsschiff "Meteor" 1925-1927, 61st Part, 2, 109-288 (in German).

Yu, Y., Chao, B. F., García-García, D., & Luo, Z. (2018), Variations of the Argentine Gyre observed in the GRACE time-variable gravity and ocean altimetry measurements. *Journal of Geophysical Research: Oceans*, *123*(8), 5375-5387.

Submitted to GEOPHYSICAL RESEARCH LETTERS

Supporting Information for "Modification of North Atlantic Deep Water by Pacific/Upper Circumpolar Deep Water in the Argentine Basin"

Sawyer V. S. Brand[1,2], Channing J. Prend[1], Lynne D. Talley[1]
[1]Scripps Institution of Oceanography, University of California San Diego, La Jolla, CA, USA
[2]University of Rhode Island, Narragansett, RI, USA

Contents of this file

1. Text S1
2. Figures S1 to S6
3. Tables S1 to S2

Text S1. Source of the low oxygen deep water in the observed anomalies. We hypothesize that the anomalously low oxygen portions of SOCCOM float profiles in the northwest Argentine Basin originated in the southeast Pacific, hence as Pacific Deep Water (PDW) that contributes to Circumpolar Deep Water (CDW) in the South Atlantic. To reach this conclusion, we considered three potential sources with low oxygen concentrations: the tropical Atlantic, southeast Pacific, and southwest Indian Ocean. We assume nearly isopycnal advection. The density of the tropical Atlantic oxygen minimum is too low (σ_2 ~35.7) to explain the low oxygen in the Argentine Basin ($\sigma_2 > 36.6$; Figure 2), and at the oxygen anomaly density, tropical Atlantic oxygen is too high (~210 µmol/kg) (Koltermann et al., 2011). Although the southwest Indian Ocean's oxygen-poor Indian Deep Water (IDW) is in the correct density range and its oxygen sufficiently low where it exits the Indian Ocean, the circulation of Agulhas waters into the South Atlantic is northwestward, reaching the Brazil Basin rather than the Argentine Basin (Reid, 1989; Beal et al., 2011). This IDW could contribute to UCDW above the Rio Grande Rise and southern Brazil Basin (e.g. Figure 2) but due to mixing with NADW, its oxygen is not low enough when it reaches the western Atlantic to create the observed extreme anomalies.

References

Beal, L., De Ruijter, W., Biastoch, A., Zahn, R., & SCOR/WCRP/IAPSOWorking Group 136, (2011). On the role of the Agulhas system in ocean circulation and climate. *Nature* 472, 429–436. https://doi.org/10.1038/nature09983

Koltermann, K. P., Gouretski, V. V., & Jancke, K. (2011), *Hydrographic Atlas of the World Ocean Circulation Experiment (WOCE). Volume 3: Atlantic Ocean* (eds. M. Sparrow, P. Chapman and J. Gould). International WOCE Project Office, Southampton, UK, ISBN 090417557X. http://woceatlas.ucsd.edu/index.html

Reid, J. L. (1989), On the total geostrophic circulation of the South Atlantic Ocean: Flow patterns, tracers and transports. *Progr. Oceanogr., 23*, 149-244.

Tarran, G. (2018), AMT 28 Cruise Report: RRS James Clark Ross (JR18-001). Atlantic Meridional Transit Project Office, Plymouth Marine Laboratory. https://www.amt-uk.org/getattachment/Cruises/AMT28/AMT_28_CRUISE_REPORT_RS.pdf (accessed 15 Jan. 2022).

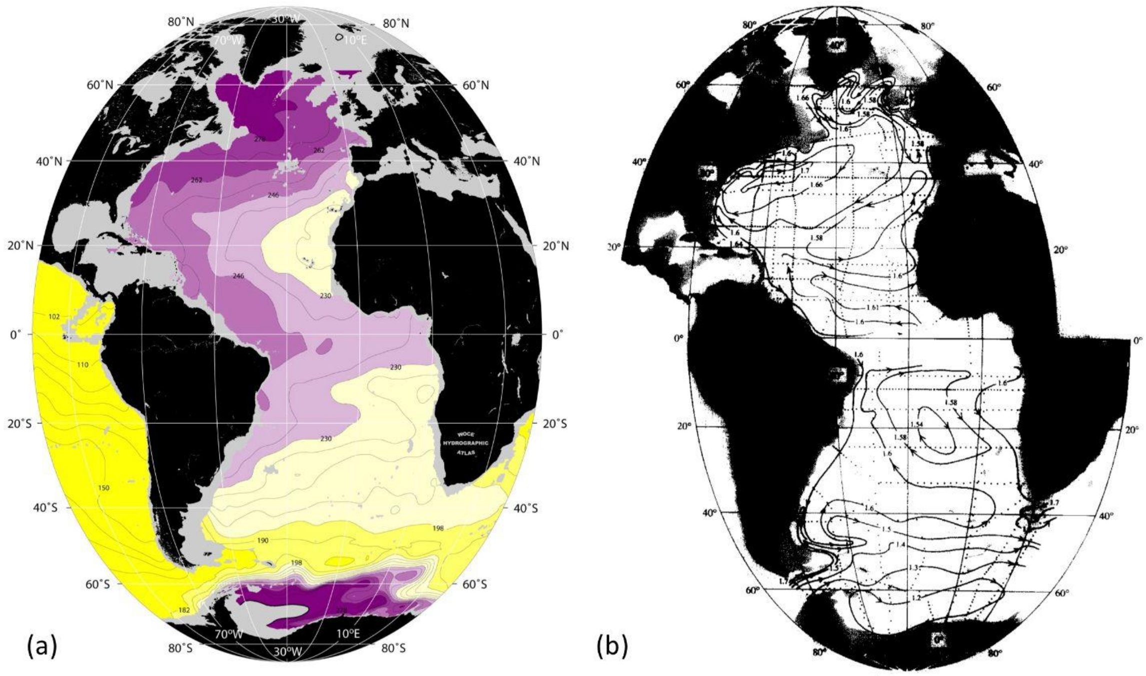

Figure S1. Oxygen on isopycnals that characterize North Atlantic Deep Water and Circumpolar Deep Water in the South Atlantic. (a) Oxygen (µmol/kg) at neutral density γ_n = 27.95 kg/m^3, reproduced from the World Ocean Circulation Experiment (WOCE) Atlantic Ocean Atlas (Koltermann et al., 2011). This surface has a depth of about 2000 m in the Argentine Basin. (b) Adjusted steric height at 1500 dbar (10 m^{2}s^{-2}), reproduced from Reid (1994).

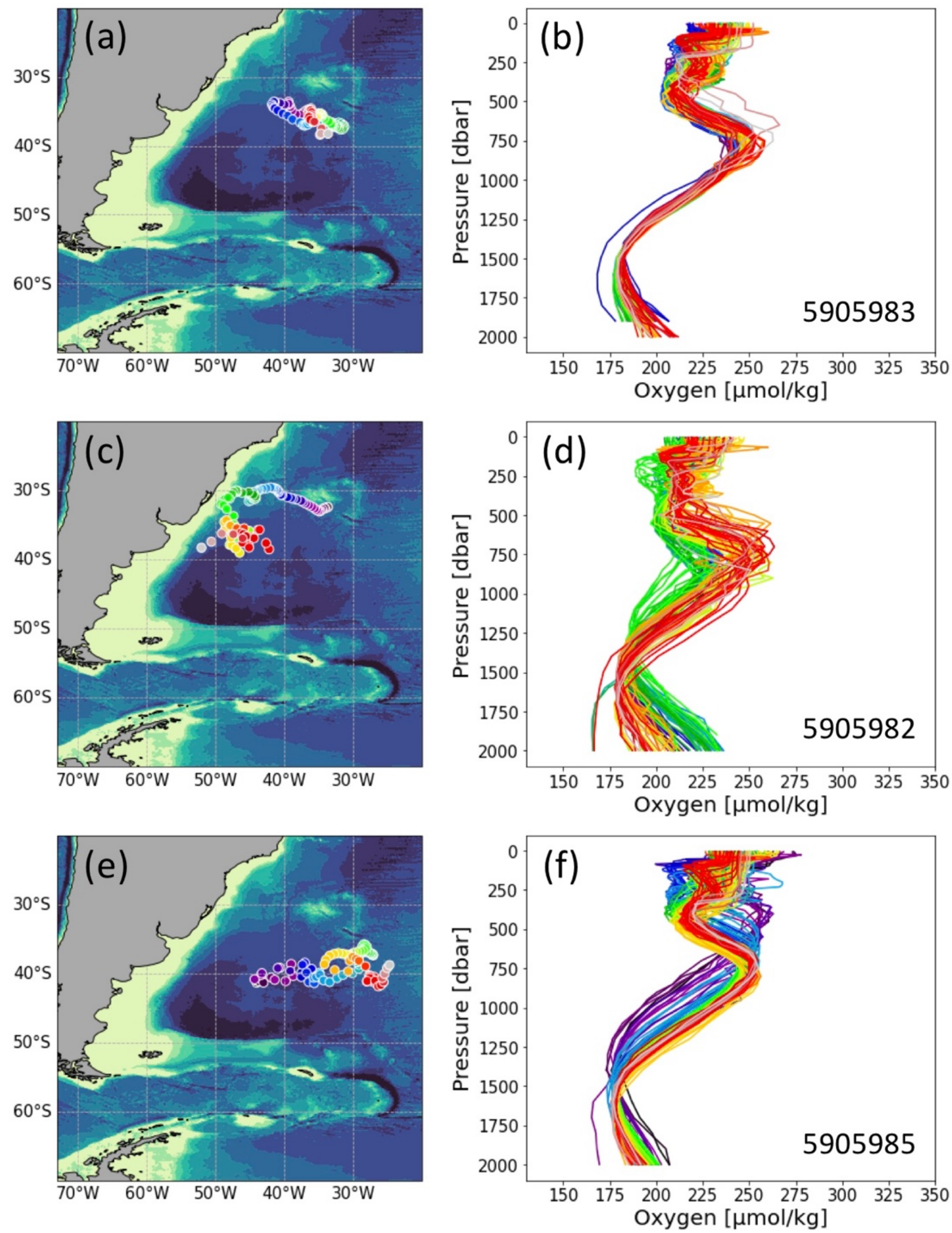

Figure S2. Trajectories (left) and dissolved oxygen profiles (right) of SOCCOM BGC Argo floats with WMO IDs of: (a, b) 5905983, (c, d) 5905982, and (e, f) 5905985. These three floats show large low oxygen anomalies within the Argentine Basin (see Figures 1 and 2). Profile and position colored by profile number.

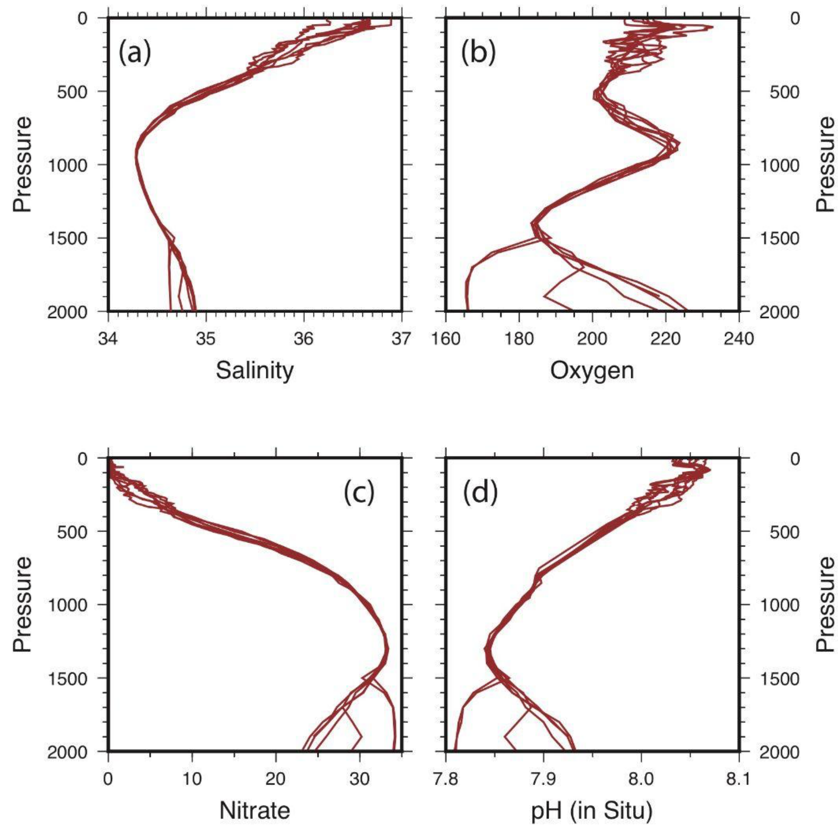

Figure S3. Quality-controlled profiles from SOCCOM BGC float 5905982 (profiles 42 through 48; 1 Dec 2019 - 5 Feb 2020) of salinity, oxygen (µmol/kg), nitrate (µmol/kg), and pH. Locations of the three profiles with large anomalies are labeled ‘2’ in Figure 2a. All positions and oxygen profiles for these floats are shown in Supplementary Figure S2b.

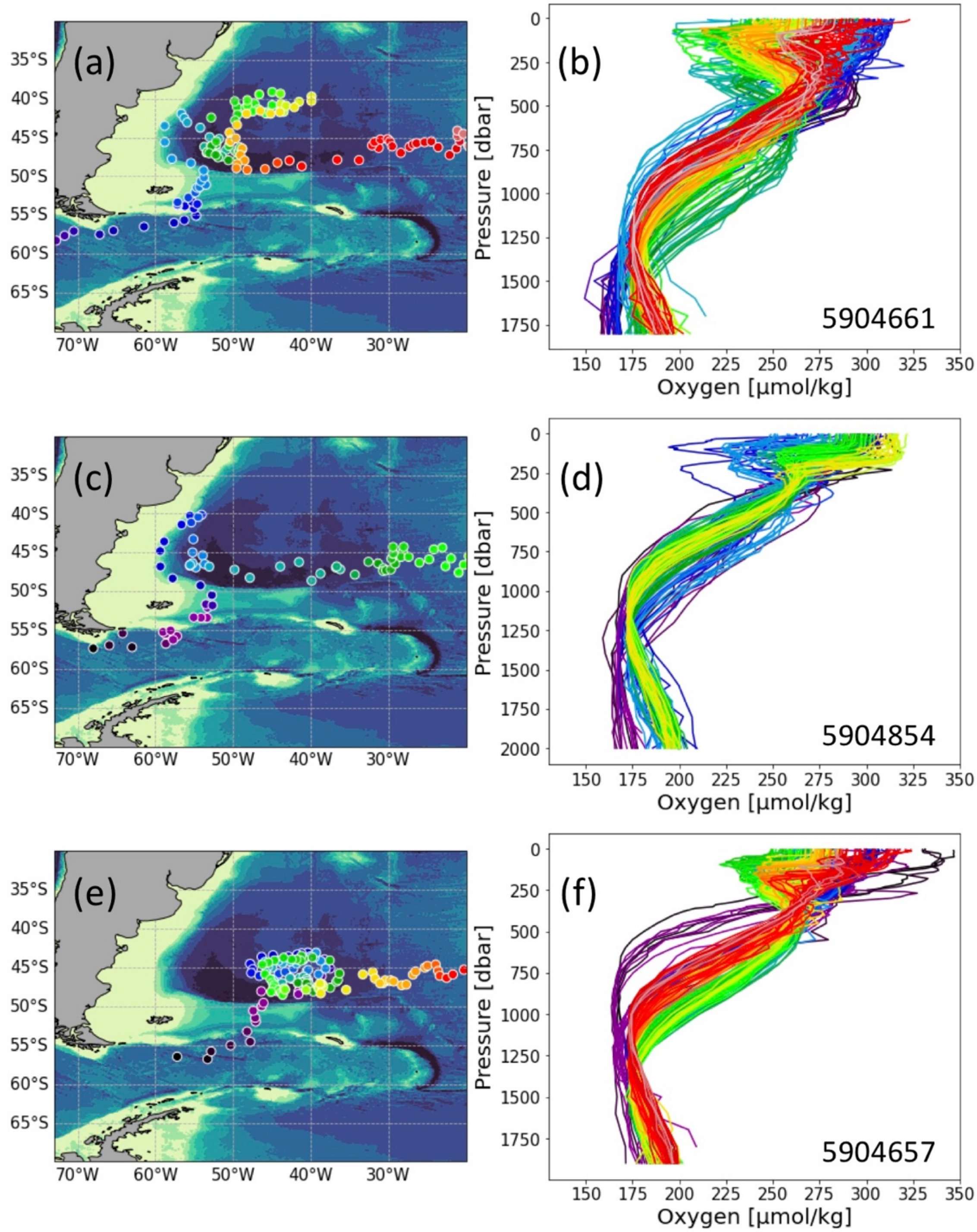

Figure S4. Trajectories (left) and dissolved oxygen profiles (right) of SOCCOM BGC Argo floats with WMO IDs of: (a, b) 5904661, (c, d) 5904854, and (e, f) 5904657. These are examples of floats from northern Drake Passage that entered the Argentine Basin and then moved eastwards. Profile and position colored by profile number.

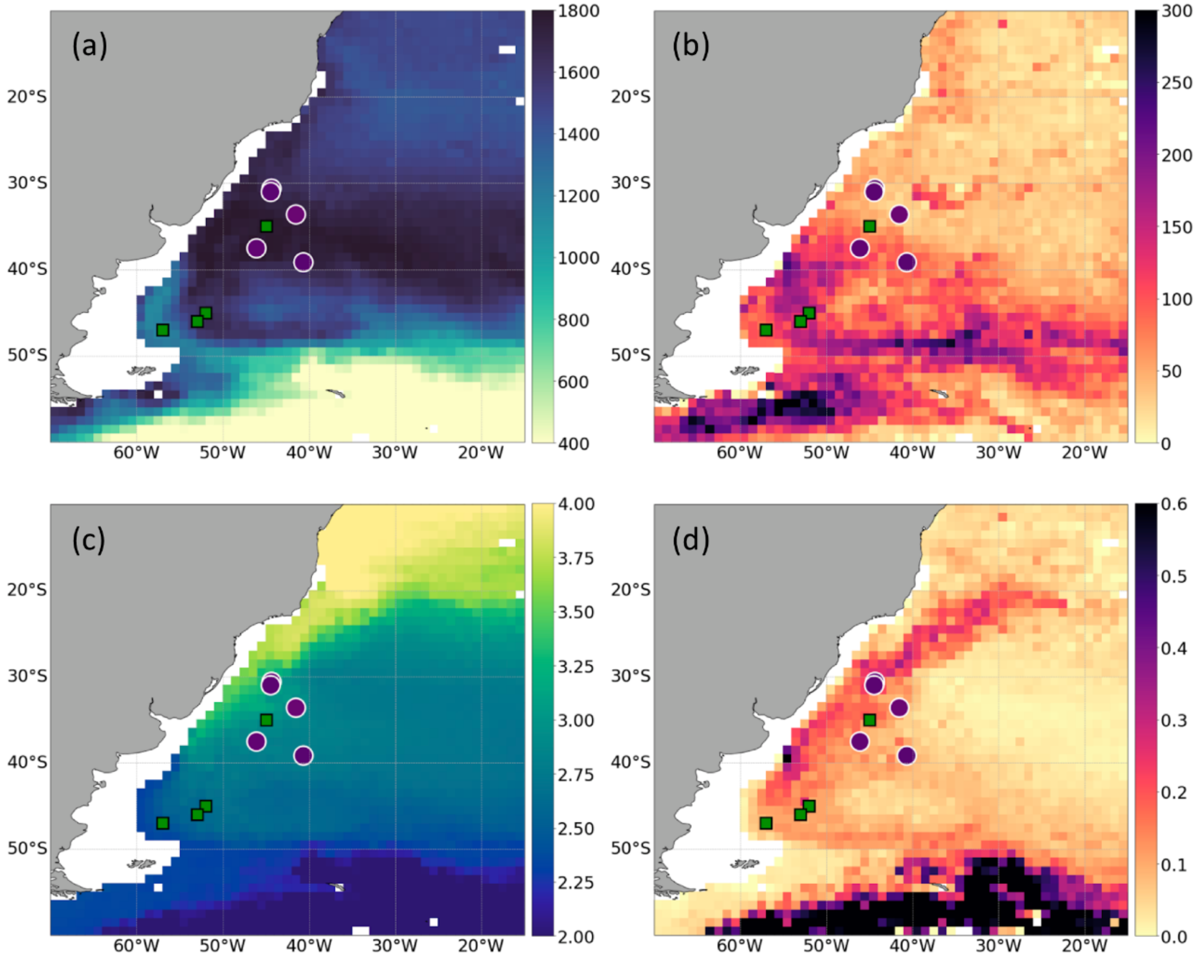

Figure S5. Pressure (top row) and conservative temperature (bottom row), in 1°x1° lat/lon bins, on the $\sigma_2 = 36.8$ kg m^{-3} surface, from all Argo profiles (years 1998 - 2020). (a) Mean pressure (dbar). (b) Standard deviation of pressure from the mean in each 1°x1° lat/lon bin. (c) Mean conservative temperature (°C). (d) Standard deviation of conservative temperature from the mean in each 1°x1° lat/lon bin.

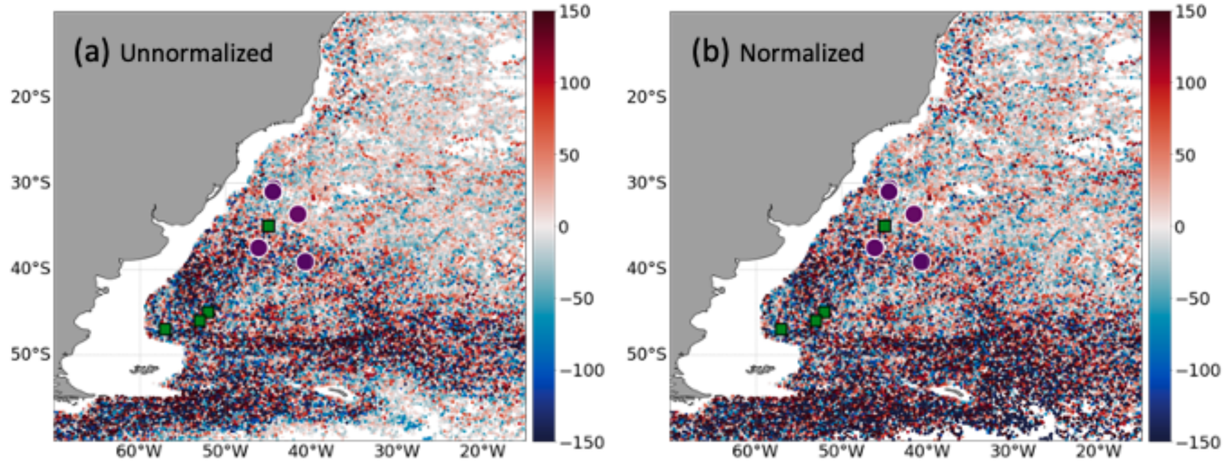

Figure S6. Pressure anomalies (dbar) from the pressure averaged in 1°x1° lat/lon bins, on the σ_2 = 36.8 kg m^{-3} surface, from all Argo profiles (years 1998 - 2020). (a) Pressure anomalies reproduced from Figure 4b. (b) Pressure anomalies normalized by stratification: $p_{norm} = p\ (N^2/N_o^2)$ where N is the local buoyancy frequency at the isopycnal, and N_o is the average buoyancy frequency over the region (30°S, 55°S) and (30°W, 65°W). $N^2 = -(g/\rho)\ \Delta\rho/\Delta z$ was calculated from the density profiles using the Gibbs Seawater routine, based on the difference in potential density between two seawater parcels, $\Delta\rho$, separated by a small vertical distance Δz, with the reference pressure taken as the midpoint between the two parcels. The purple circles and green squares are oxygen anomalies and historically identified abyssal eddies, as in Figure 4.

Table S1. Oxygen, temperature, and salinity anomaly magnitudes for large low oxygen anomalies on SOCCOM BGC Argo profiles in the northern Argentine Basin (Figures 3, S2 and S3). Mean and standard deviation are with respect to all profiles from the given float. These floats were deployed from the RRS JC Ross AMT28 cruise (Tarran, 2018).

Float WMO ID	Pro-file #	Lat.	Long.	Date	Density σ_2 at lowest oxygen (kg/m^3)	Mean oxygen at that density (µmol/kg)	Standard deviation at that density (µmol/kg)	Oxygen at lowest oxygen (µmol/kg)	Oxygen anomaly at lowest oxygen (µmol/kg)	Depth and density σ_2 at top of anomaly
5905982	42	30.82 °S	44.35 °W	11/27/2019	36.85	203.61	13.36	165.51	-27.51	1500 m 36.73
5905982	45	31.01 °S	44.45 °W	12/27/2019	36.86	207.20	13.73	165.83	-51.6	1500 m 36.75
5905982	94	37.55 °S	46.10 °W	5/03/2021	36.80	193.14	10.63	166.64	-18.8	1700 m 36.6
5905983	17	33.62 °S	41.52 °W	3/22/2019	36.76	180.71	2.01	168.29	-12.43	1000 m 36.62
5905985	6	39.18 °S	40.65 °W	12/04/2018	36.86	192.13	3.23	165.20	-25.93	1400 m 36.78

(cont.)

Float WMO ID	Profile #	Density σ_2 at lowest oxygen	Mean temperature at that density (°C)	Standard deviation at that density (°C)	Temperature anomaly at lowest oxygen (°C)	Mean salinity at that density	Standard deviation at that density	Salinity anomaly at lowest oxygen
5905982	42	36.85	3.1	0.3	-0.89	34.95	0.06	-0.21
5905982	45	36.86	3.2	0.4	-1.02	34.98	0.07	-0.18
5905982	94	36.80	3.1	0.3	-0.77	34.88	0.06	-0.12
5905983	17	36.76	2.800	0.04	-0.32	34.780	0.006	-0.06
5905985	6	36.86	2.78	0.04	-0.58	34.905	0.008	-0.11

Table S2. Additional SOCCOM BGC profiles with large negative or positive oxygen anomalies below 1000 m and large-layered vertical structure (Figure 1). All of these floats were deployed in the Pacific and entered the Argentine Basin through Drake Passage. All anomalies were located in either the Malvinas/Brazil Current Confluence (MBC) or between Zapiola Rise and the Falkland Escarpment (ZRFE).

Float WMO ID	Pro-file #	Lat.	Long.	Date	Type of oxygen anomaly	Loca-tion	Local background oxy at that density	Oxygen at extreme oxygen	Oxygen anomaly	Depth and density σ_2 at top of anomaly
5906216	35	47.59 °S	42.27 °W	12/06/2020	Low oxygen, full profile (not layered)	ZRFE	176 µmol/kg	165.9 µmol/kg	-10.1 µmol/kg	1480 m 36.83 σ_2
5906216	37	46.75 °S	33.88 °W	12/26/2020	Low oxygen intrusion	ZRFE	176 µmol/kg	168.1 µmol/kg	-7.9 µmol/kg	1600 m 36.85 σ_2
5906217	59	47.36 °S	41.76 °W	08/16/2021	Low oxygen layering	ZRFE	188 µmol/kg	168.4 µmol/kg	-19 µmol/kg	1777 m 36.821 σ_2 Min at 1875 m 36.846 σ_2
5906217	60	48.18 °S	39.11 °W	08/27/2021	Low oxygen layering	ZRFE	178 µmol/kg	169.0 µmol/kg	-9 µmol/kg	1480 m 36.77 σ_2 Min at 1580 m 36.806 σ_2
5906217	65	43.91 °S	37.67 °W	10/17/2021	Low oxygen deep layer	ZR	185 µmol/kg	166.9 µmol/kg	-18.1 µmol/kg	1600 m 36.833 σ_2 Min at 1875 m 36.886 σ_2
5906217	40	39.83 °S	54.24 °W	02/02/2021	Low oxygen profile with heave. High oxygen	MBC	176 µmol/kg	166.3 µmol/kg	-10 µmol/kg	Break to higher oxygen below 1600 m 36.791 σ_2

					layer at bottom					
5904661	51	43.08 °S	55.91 °W	05/29/2017	High oxygen	MBC	175 µmol/kg	215 µmol/kg	40 µmol/kg	1000 m 36.75 σ_2
5904854	26	41.13 °S	55.39 °W	09/05/2017	High oxygen, interleav-ing	MBC	185 µmol/kg	207 µmol/kg	22 µmol/kg	1100 m 36.76 σ_2
5905079	111*	42.13 °S	55.37 °W	03/08/2020	High oxygen	MBC	185 µmol/kg	218 µmol/kg	33 µmol/kg	1180 m 36.766 σ_2
5905079	112*	42.83 °S	54.83 °W	03/18/2020	High oxygen, layered	MBC	180 µmol/kg	202 µmol/kg	20 µmol/kg	1180 m 36.758 σ_2
5904657	13	48.01 °S	44.44 °W	05/13/2016	High oxygen	ZRFE	172 µmol/kg	210 µmol/kg	28 µmol/kg	1400 m 36.871 σ_2

*Latitude and longitude linearly interpolated.